Compact disposal of high-energy electron beams using passive or laser-driven plasma decelerating stage

A. Bonatto, C. B. Schroeder, J.-L. Vay, C. R. Geddes, C. Benedetti, E. Esarey and W. P. Leemans

Lawrence Berkeley National Laboratory, Berkeley, CA, 94720, USA

Abstract. A plasma decelerating stage is investigated as a compact alternative for the disposal of high-energy beams (beam dumps). This could benefit the design of laser-driven plasma accelerator (LPA) applications that require transportability and / or high-repetition-rate operation regimes. Passive and laser-driven (active) plasma-based beam dumps are studied analytically and with particle-in-cell (PIC) simulations in a 1D geometry. Analytical estimates for the beam energy loss are compared to and extended by the PIC simulations, showing that with the proposed schemes a beam can be efficiently decelerated in a centimeter-scale distance.

Keywords: laser-plasma accelerators, beam dump, energy loss, beam deceleration
PACS: 52.38.Kd, 52.40.Mj

INTRODUCTION

Laser-driven plasma-based accelerators (LPAs) provide a compact way to produce high-energy electron beams [1–3], but conventional techniques for the disposal of such beams can require large and heavy beam dumps that limit the compactness of the overall accelerator system. A plasma-based decelerating stage may greatly reduce the required size of the beam dump by reducing beam energy. Since the deceleration is achieved by collective fields rather than by scattering, high-energy radiation is not produced during this process. Previous 3D PIC simulations [4, 5] demonstrated that a plasma-based scheme could be used for deceleration with the same efficacy obtained for acceleration in an LPA, provided that the beam is at the proper wakefield phase.

In this work we derive an analytical model to study the energy loss of an electron beam propagating in a plasma in the linear regime. This is done from first principles, for a 1D geometry. The investigation is complemented with the aid of particle-in-cell (PIC) simulations, which are useful for benchmark purposes and also to extend the analysis beyond the validity of the derived model. Two cases, passive and active dumping, are presented and compared. In the passive dumping case, a highly-relativistic electron beam propagates in an initially quiescent plasma, exchanging energy with the self-excited wakefield. This scenario, usually approached as a scheme to excite a wakefield to accelerate a second witness [6–8], is studied here emphasizing the energy loss of the beam as it propagates. In the active case the beam propagates in the wake of a laser pulse, experiencing a net electric field that is a superposition of the self-excited and laser-driven wakefields. As it is shown in this paper, plasma-based dumping schemes can decelerate high-energy electron beams to non-relativistic velocities after a few centimeters of propagation in the plasma.

WAKEFIELD EXCITATION

The excitation of wakefields driven either by laser pulses or electron beams in plasma-based accelerators is well documented in the literature [1–3, 6–9]. In the following we consider a 1D geometry. If the amplitude of such fields is small when compared to the cold non-relativistic wave breaking electric field $E_0 = c\, m_e \omega_p / e$ [9], where c is the speed of light in vacuum, $\omega_p = k_p c = (4\pi n_0 e^2/m_e)^{1/2}$ is the electron plasma frequency, n_0 is the background electron plasma density and m_e and e are the electron mass and charge respectively, then the system evolves in the linear regime. In this 1D, linear regime, the plasma density perturbation $\delta n/n_0 \equiv (n-n_0)/n_0$ and electric field E_z/E_0 are given by

$$(\partial_\xi^2 + k_p^2)\,\delta n/n_0 = -k_p^2\,(n_b/n_0) + \partial_\xi^2 (a^2/2), \tag{1}$$

$$(\partial_\xi^2 + k_p^2)\,(E_z/E_0) = -k_p\,\partial_\xi (n_b/n_0) - k_p \partial_\xi (a^2/2), \tag{2}$$

where $\zeta \equiv z - ct$ is the coordinate in the co-moving frame, n_b is the electron beam number density and $a \equiv eA/m_e c^2$ is the vector potential describing the laser pulse. Considering the quasi-static approximation, the set of Eqs. (1)-(2) can be solved using the proper Green's Function to obtain the following analytical solution for the wakefield:

$$E_z/E_0 = -k_p \int_{\infty}^{\zeta} d\zeta' \cos[k_p(\zeta - \zeta')]\,(n_b/n_0 + a^2/2). \tag{3}$$

Eq. (3) can be used to calculate the wakefield generated by an electron beam and/or laser pulse with arbitrary profiles, provided that their amplitudes remain small enough to ensure that $E_z/E_0 \ll 1$.

PASSIVE BEAM DUMP

To investigate the energy loss of a highly-relativistic electron beam going through a plasma-based decelerating stage, we consider the rate of energy change in the beam is due to the longitudinal wakefield acting on it, $d\gamma/ds \simeq -k_p E_z/E_0$, where $s \equiv ct$ is the propagated distance in the plasma. In the passive dumping scheme, the plasma is initially quiescent and the beam only experiences its self-excited wakefield. Since the beam reaches the decelerating stage with high-energy, it is initially very stiff and therefore its shape does not change as it propagates. Under this assumption, valid while the beam remains highly-relativistic, the electric field becomes a function of the co-moving coordinate ζ only, $E_z = E_z(\zeta)$, and the integration of the equation of motion yelds the following expression for the relativistic factor

$$\gamma(\zeta, s) = \gamma_0 - k_p\, s\, [E_z(\zeta)/E_0]\,. \tag{4}$$

Once $\gamma(\zeta, s)$ is known, the normalized total energy of the beam $U(s) = \int d\zeta\, \gamma(\zeta, s)\, n_b(\zeta)/n_0$ can be calculated. For a beam with $\gamma(\zeta, 0) = \gamma_0$, the initial energy is given by $U(s=0) = U_0 = \gamma_0 \int d\zeta\, n_b(\zeta)/n_0$. Then, from Eq. (4) we can derive an expression for the beam energy,

$$\frac{U(s)}{U_0} = 1 - s\,\frac{k_p \int d\zeta\, [E_z(\zeta)/E_0]\, [n_b(\zeta)/n_0]}{\gamma_0 \int d\zeta\, n_b(\zeta)/n_0}, \tag{5}$$

which holds for beams with arbitrary longitudinal profiles. For a flat-top beam, for example, $n_b(\zeta)/n_0 = n_b/n_0$ for $0 \le \zeta \le L$ and zero otherwise, by using Eqs. (3) and (5) the energy is $U/U_0 = 1 - k_p s\{(n_b/n_0)[1 - \cos(k_p L)]/(\gamma_0 L)\}$. For a half-sine beam, $n_b(\zeta)/n_0 = (n_b/n_0)\sin(\pi\zeta/k_p L)$ if $0 \le \zeta \le L$ and zero otherwise, the beam energy is

$$\frac{U(s)}{U_0} = 1 - s\,\frac{\pi^3 k_p^2 L\,(n_b/n_0)\cos\,(k_p L/2)^2}{\gamma_0(\pi^2 - k_p^2 L^2)^2}. \tag{6}$$

The passive dumping scheme is also investigated numerically by means of 1D PIC simulations using the code Warp [10], which self-consistently calculates the beam phase space and wakefield as it propagates. In particular, the beam energy loss obtained from the simulation is compared to the analytical solution calculated with Eq. (6). Results are presented in Fig. 1. In the simulation we consider a half-sine beam with normalized density peak $n_b/n_0 = 0.1$, length $L = 8.4\,\mu$m and uniform initial relativistic factor $\gamma_0 = 500$, propagating in a plasma with background density $n_0 = 3 \times 10^{17}\text{cm}^{-3}$. These parameters are suitable to investigate the energy loss in the linear regime. Fig. 1(a) shows the spatial configuration of the beam (represented as a red line) and the wakefield E_z/E_0 at the beginning of the propagation ($s \simeq 0.7$ cm). Fig. 1(b) shows the phase space at this point, with the normalized energy $\gamma/\gamma_0 \simeq 1$ along the beam. As the plasma is initially quiescent and the beam is short ($k_p L \le \pi/2$), the electric field E_z/E_0 rises from zero at the head ($k_p\zeta = 0$) to its maximum value along the beam at its tail. For this reason, even though the total energy loss is a linear function of the propagated distance s, beam particles closer to the tail lose energy faster than those closer to the head. As a consequence, the tail becomes non-relativistic while the head still preserves most of the initial energy, causing a rapid lengthening of the beam. The PIC simulation shows this behavior, which is not captured by our model. Fig. 1(c) shows that at $s \simeq 9.5$ cm the beam becomes long enough to reach the accelerating phase and Fig. 1(d) confirms that, when this happens, $\gamma/\gamma_0 \ll 1$ near the beam tail while $\gamma/\gamma_0 \sim 1$ at the head. For the given parameters, a passive decelerating stage should not be longer then 9.5 cm, since beyond this distance particles from the tail reach the accelerating phase and start gaining energy. Figures 1(e) and 1(f) show that at $s \simeq 17$ cm the tail regained almost half of its initial energy ($\gamma/\gamma_0 \sim 0.5$). The last panel of Fig. 1, panel (g), shows the normalized total energy U/U_0 as a function of the propagated distance s. While the beam remains relativistic ($\gamma/\gamma_0 \simeq 1$), the energy loss is linear and the

agreement between the PIC simulation (solid line) and the analytical solution calculated from Eq. (6) (dashed line) is excellent. Once the tail becomes non-relativistic, the evolution of the beam shape as it propagates in the plasma cannot be neglected and the linear approximation for the energy loss does not hold. This explains why the energy loss from the PIC simulation departs from the linear analytical model after $s \simeq 9.5\,\mathrm{cm}$. After this point the total energy remains approximately constant, $U/U_0 \simeq 0.38$, due to the balance between energy gain and loss shown in Figures 1(e) and 1(f).

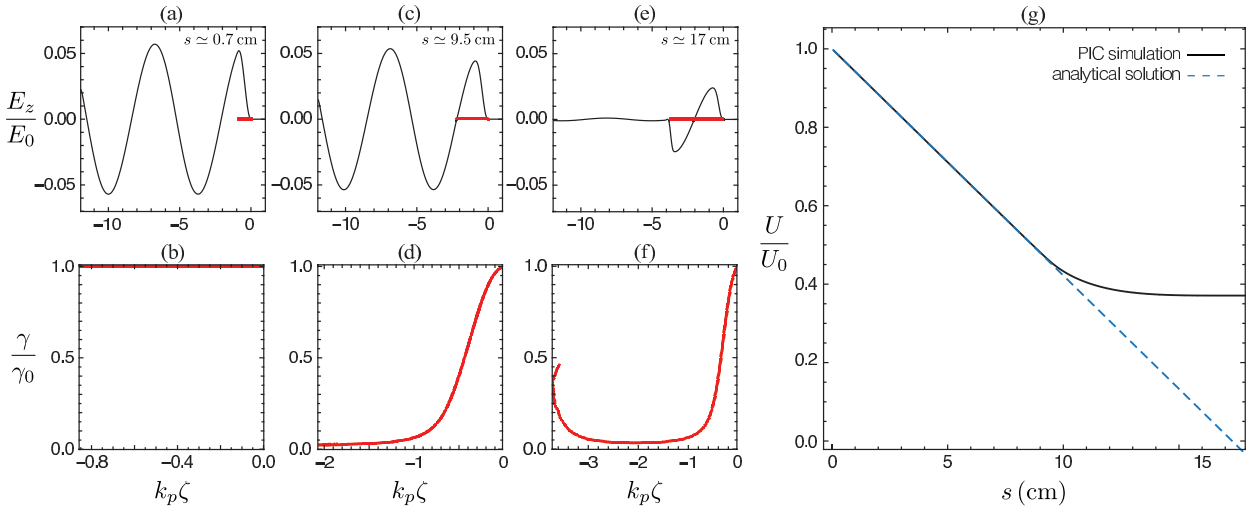

FIGURE 1. (Color online) Passive dumping. An electron beam (red line) with density peak $n_b/n_0 = 0.1$, length $L = 8.4\,\mu m$ and $\gamma_0 = 500$ propagates in an initially quiescent plasma with density $n_0 = 3 \times 10^{17}\mathrm{cm}^{-3}$, transferring energy to the self-excited electric wakefield. Panel (a) shows the beam and wakefield E_z/E_0, and panel (b) shows the normalized energy γ/γ_0, both at $s \simeq 0.7\,\mathrm{cm}$. While the beam is short ($k_pL \leq \pi/2$), E_z/E_0 rises from zero at its head ($k_p\zeta = 0$) to its maximum inside the beam at its tail. As a consequence, beam particles located closer to the tail lose energy faster than those closer to the head, causing the lengthening of the beam toward the accelerating phase of the wakefield. Panels (c) and (d) show this happening at $s \simeq 9.5\,\mathrm{cm}$. After this point, the beam length keeps growing and particles experiencing the accelerating field start to gain energy, as shown in panels (e) and (f) plotted at $s \simeq 17\,\mathrm{cm}$. Panel (g) shows the history of the normalized total energy U/U_0. While the particles are highly-relativistic, the agreement between the Warp PIC simulation (solid line) and the analytical solution (dashed line) is excellent. When the beam reaches the accelerating phase of the wakefield ($s \simeq 9.5\,\mathrm{cm}$), the maximum energy loss is achieved.

ACTIVE BEAM DUMP

The smallness of the beam wakefield at its head, which constrains the effectiveness of the passive dumping scheme, can be overcome in the active dumping scheme by the excitation of a laser-driven wakefield overlapping the beam in the plasma. By setting the laser amplitude a_0 and the beam injection phase one can control the electric field amplitude and gradient experienced by the whole beam.

The model for the active scheme is developed from the same equation of motion mentioned in the previous section, $d\gamma/ds \simeq -k_pE_z/E_0$, but considering now the electric field as a combination of two components, $E_z(\zeta,s) = E_z(\zeta) + E_{zl}(\zeta,s)$, where $E_z(\zeta)$ is the beam-driven wakefield derived from Eq. (3), and $E_{zl}(\zeta,s)$ is the wakefield excited by the laser,

$$E_{zl}(\zeta,s) = \frac{E_{zl}}{E_0}\sin\left(k_p\zeta + \frac{k_ps}{2\gamma_g^2}\right). \tag{7}$$

Eq. (7) is obtained considering that in the linear regime ($a^2 < 1$) a sinusoidal plasma wave is excited by the laser. For a circularly polarized laser pulse with a Gaussian envelope $a^2 = a_0^2\exp(-\zeta^2/\sigma^2)$ and $\sigma = \lambda_p/\sqrt{2}\pi$ [2], the amplitude of the wakefield is given by $E_{zl}/E_0 \simeq 0.76\,a_0^2$. Since the beam is highly-relativistic, it propagates faster than the laser pulse in the plasma and thus the phase slippage [2] between both cannot be neglected. This effect is taken in account in Eq. (7) by the term $k_ps/2\gamma_g^2$, where γ_g is the relativistic factor associated with the laser group velocity v_g. Including

the laser-generated wake Eq. (7), the expression for the energy of a beam with a half-sine profile in the active dumping scheme is

$$\frac{U(s)}{U_0} = 1 - s\frac{\pi^3 k_p^2 L\,(n_b/n_0)\cos(k_p L/2)^2}{\gamma_0(\pi^2 - k_p^2 L^2)^2} + \frac{4\pi^2\gamma_g(E_{zl}/E_0)\cos(k_p L/2)}{\gamma_0(k_p^2 L^2 - \pi^2)}\sin\left(\frac{k_p s}{4\gamma_g^2}\right)\sin\left(\frac{k_p L}{2} + \frac{k_p s}{4\gamma_g^2}\right). \quad (8)$$

Our investigation is complemented with a PIC simulation performed with the same parameters as those of the previous section but with a laser pulse propagating in front of the beam. The laser strength parameter $a_0 \simeq 0.38$ is chosen to excite a wakefield with an amplitude comparable to that of the beam. The relative initial phase between the beam and laser wake is chosen in such a way that the tail of the former is aligned with the beginning of a decelerating phase of the latter. At this phase, the beam would be simultaneously focused in a 3D geometry. The evolution of the electric field and beam phase space, as well as the energy loss from the simulation compared to the analytical solution Eq. (8), are presented in Fig. 2.

Fig. 2(a), plotted at $s \simeq 0.02$ cm, shows the initial phase of the beam (red line) and laser wake, and Fig. 2(b) shows the phase space. Due to the deceleration, γ decreases and the phase slippage toward the laser pulse is progressively reduced as the beam propagates. Then, depending on its initial energy, the beam can either slip through the decelerating phase and reach an acceleration region ahead of it, or become slower than the pulse ($\gamma < \gamma_g$) before crossing the deceleration region, slipping backward. The PIC simulation shows that this is the behavior observed for the chosen parameters and, together with beam lengthening, it limits the distance over which it propagates losing energy. Fig. 2(c) shows the spatial configuration of the beam and the wakefield at $s \simeq 5.8$ cm, where the minimum value for the normalized energy, $U/U_0 \simeq 0.03$, is observed. Fig. 2(d) exhibits an almost flat phase space profile, with $\gamma/\gamma_0 \ll 1$, resulting from a more homogeneous beam energy extraction in the active dumping scheme. Figures 2(e) and 2(f), plotted at $s \simeq 8$ cm, show that for longer distances the beam starts to gain energy.

Despite the 1D geometry, the qualitative behavior presented in Fig. 2 and discussed in this section can be used to describe the physics of laser-driven dumping schemes in 3D [4, 5] while the beam is contained in a focusing phase of the transverse wakefield.

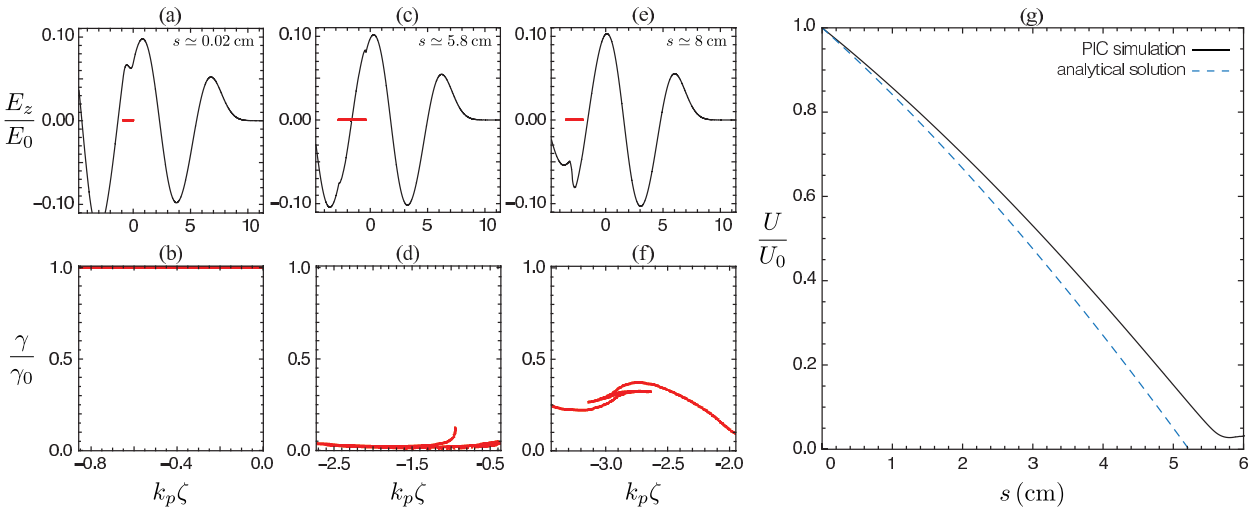

FIGURE 2. (Color online) Active dumping. An electron beam (red line) with density peak $n_b/n_0 = 0.1$, length $L = 8.4\,\mu m$ and initial energy $\gamma_0 = 500$ (for each electron) is injected in a wakefield excited by a laser pulse with $a_0 \simeq 0.38$, in a plasma with density $n_0 = 3 \times 10^{17}\text{cm}^{-3}$.Panel (a) shows the beam loaded in the laser wakefield at the proper phase for the entire beam to be decelerated. Panel (b) shows the initial phase space. The phase slippage that happens because the beam is faster than the laser pulse is progressively reduced due to the deceleration. For the given parameters, the beam loses energy and becomes non-relativistic before slipping through the the decelerating phase of the wakefield. When this happens, the lengthening and the inversion of the phase slippage direction causes the beam to reach the accelerating phase of the electric field. Panels (c) and (d) depict the spatial configuration and the phase space at $s \simeq 5.8$ cm, where the maximum energy loss occurs. After this distance, the beam starts to gain energy from the accelerating field as shown in panels (e) and (f), plotted at $s \simeq 8$ cm. Panel (g) shows the history of the total energy loss normalized by the initial energy, U/U_0, calculated by PIC simulation (solid line) and the analytical solution (dashed line). Differences between the simulation and analytic solution are attributed to non-linearities in the wakefield for $a_0 = 0.38$. At $s \simeq 5.8$ cm the beam energy has the minimum value observed, $U/U_0 \simeq 0.028$. Beyond this point, the beam gains energy from wakefield and is accelerated.

CONCLUSIONS

Plasma-based dumping schemes are a promising technique for reducing the energy of highly-relativistic beams over centimeter-scale distances. These schemes could be used to drastically reduce the size of conventional dumping structures, thereby improving the overall compactness of LPAs and making them more suitable for the design of transportable applications, such as sources of quasi-monoenergetic photon beams [4]. High-repetition-rate LPA facilities could also take advantage of this technique to mitigate the huge beam dumps required to operate safely in such regime. In this paper, passive and active dumping schemes were investigated with the aid of analytical models and PIC simulations in a 1D geometry. In a passive decelerating stage, the beam lost approximately 62% of its initial energy after propagating 9.5 cm for the example considered. For the same parameters, approximately 97% of the initial energy was depleted in the active scheme after 5.8 cm of propagation. The improvement of the active over the passive dumping can be clearly understood if one compares Fig. 1(d) with Fig. 2(d): both panels depict the beam phase space when the maximum energy losses were achieved and, while the energy at the head of the beam was preserved in the former scheme, it was mostly depleted in the latter.

The results presented in this work are preliminary. Optimizations for improving the total energy loss in the passive dumping scheme (which is simpler to implement experimentally) and for reaching the maximum energy depletion in shorter distances in the active case (to avoid the need of a plasma channel to guide the laser) are under investigation. Plasma tapering to increase the deceleration length, studies to determine the optimal parameters (phasing, laser intensity, beam loading effects) and the combination of passive and active deceleration are among the options to achieve such improvements.

ACKNOWLEDGMENTS

This work was supported by the U.S. Dept. of Energy Office of Science Office of High Energy Physics, under Contract No. DE-AC02-05CH11231, by the National Nuclear Security administration DNN/NA-22 and by the CAPES Foundation of Ministry of Education of Brazil, under Process No. 10743-13-8, and used the computational facilities at the National Energy Research Scientific Computing Center (NERSC).

REFERENCES

1. Tajima, T., and Dawson, J. M., *Phys. Rev. Lett.*, **43**, 267–270 (1979).
2. Esarey, E., Schroeder, C. B., and Leemans, W. P., *Rev. Mod. Phys.*, **81**, 1229–1285 (2009).
3. Leemans, W. P., Nagler, B., Gonsalves, A. J., Tóth, C., Nakamura, K., Geddes, C. G. R., Esarey, E., Schroeder, C. B., and Hooker, S. M., *Nature Phys.*, **2**, 696–699 (2006).
4. Vay, J.-L., Geddes, C. G. R., Rykovanov, S. G., Schroeder, C. B., Esarey, E., and Leemans, W. P., *Proceedings of NPNSNP* (submitted, 2014).
5. Rykovanov, S. G., Geddes, C. G. R., Vay, J. L., Schroeder, C. B., Esarey, E., and Leemans, W. P., *J. Phys. B* (submitted, 2014).
6. Chen, P., Dawson, J. M., Huff, R. W., and Katsouleas, T., *Phys. Rev. Lett.*, **54**, 693–696 (1985).
7. Rosenzweig, J. B., Cline, D. B., Cole, B., Figueroa, H., Gai, W., Konecny, R., Norem, J., Schoessow, P., and Simpson, J., *Phys. Rev. Lett.*, **61**, 98–101 (1988).
8. Blumenfeld, I., Clayton, C. E., Decker, F.-J., Hogan, M. J., Huang, C., Ischebeck, R., Iverson, R., Joshi, C., Katsouleas, T., Kirby, N., Lu, W., Marsh, K. A., Mori, W. B., Muggli, P., Oz, E., Siemann, R. H., Walz, D., and Zhou, M., *Nature*, **445**, 741–744 (2007).
9. Dawson, J. M., *Phys. Rev.*, **113**, 383–387 (1959).
10. Vay, J.-L., Grote, D. P., Cohen, R. H., and Friedman, A., *Computational Science and Discovery*, **5**, 014019 (2012).